Journal Homepage: - www.journalijar.com

INTERNATIONAL JOURNAL OF ADVANCED RESEARCH (IJAR)

Article DOI: 10.21474/IJAR01/16885
DOI URL: http://dx.doi.org/ 10.21474/IJAR01/16885

RESEARCH ARTICLE

MINERAL EXPLORATION IN THE VICINITY OF THE LATE EDIACARAN BOUTEGLIMTAPLITE AND PEGMATITE DIKES INIMITER INLIER USING ASTER DATA: PRELIMINARY RESULTS

Mehdi Ousbih[1], MohaIkenne[1], FatihaAskkour[1], Mouna Id-Belqas[1], Ikirri Mustapha[1], Abdessamad El Atillah[2], Mohamed Mahmoud Sebbab[3] and Bouchra Baidada[4]

1. Department of Geology, Faculty of Sciences, Ibnou Zohr University, BP. 8016, Agadir, Morocco.
2. Regional Directorate of Energy and Mines of Agadir, Ministry of Energy Transition and Sustainable Development. Mohammed V Avenue, 80000, Agadir, Morocco.
3. Department of Geography and Planning, Faculty of Languages, Arts and Humanities- AitMelloul, IbnouZohr University, AitMelloul 80000, Morocco.
4. Ecole Nationale de Technologie, FkihBensalah, MoulaySlimane University, Beni-Mellal, Morocco.

Manuscript Info

Manuscript History
Received: 10 March 2023
Final Accepted: 14 April 2023
Published: May 2023

Key words:-
ASTER, Field data, Mineralization, Pegmatite, Aplite, Imiter Inlier

Abstract

In the southern part of the Imiter inlier, the early Ediacaran basement of the Saghro Group is crosscut by an important swarm of aplitic and pegmatitic dikes that display an extension of several meters and which can exceed 10 in thickness. They are distributed according to two main directions: NE-SW and NW-SE. Petrographic analysis reveals that the pegmatites and aplite primarily consist of quartz, plagioclase, K-feldspar, muscovite, biotite, allanite, and sphene. The BouTeglimt pegmatites, related to the large BouTeglimt granitic and granodioritic plutons, are exterior pegmatites type, hosted in the metamorphic country rocks. Pegmatite zoning is recognized at two scales: internal zoning, representing variations in mineralogy and texture within individual pegmatite bodies, and regional zoning, characterized by increased mineralogical complexity with distance from the granitic source. Using the ASTER sensor, the study investigated significant clayey, phyllitic, and propylitic alterations of the pegmatites, aplite, and their host rocks in the Imiter mine area. Field investigations and mineralogical characterization highlight four new mineralized zones in base and precious metals. These zones are commonly situated at the peripheries of granites or at the contact between the SG series and the late Ediacaran rocks of the Ouarzazate Group. The mineralization is observed in steeply-dipping veins along major E-W faults parallel to the Imiter fault, as well as in stockwork ore within tuffs, lapilli tuff, rhyolite, and disseminated mineralization within various Ouarzazate Group pyroclastic rocks. The ore mineralogy comprises sulfides and oxide minerals. Furthermore, the muscovite-rich BouTeglimt pegmatite and aplite can be considered an excellent exploration indicators due to their occurrence in fertile granites and rare-element pegmatites. They may hold potential as indicators of tantalum mineralization.

Corresponding Author:- Mehdi Ousbih
Address:- Department of Geology, Faculty of Sciences, Ibnou Zohr University, BP. 8016, Agadir, Morocco.

Introduction:-

Pegmatites and aplites are highly differentiated rocks that outcrop as dikes and occur respectively as coarse-grained or very fine grain size rocks, associated with igneous or with metamorphic rocks. They are assumed to represent the final result of the magmatic differentiation. These highly differentiated rocks have the potential to accumulate significant concentrations of economically valuable elements such as Li, Cs, Nb, Ta, and the rare earth elements (REE), as well as several other commodities including Sn, Rb, Be, W, and Au (London, 2016). The study of pegmatites holds both scientific and economic significance. Within the scientific community, pegmatites and aplites have sparked numerous debates, particularly regarding their classification and origin (Dill et al., 2015). From an economic standpoint, it has been observed that the most valuable pegmatites tend to be enriched in incompatible elements, which encompass high-field strength and large ion lithophile elements. These elements often include metal ores of considerable economic importance (Linnen, 2012). Apart from their strategic metal resources, pegmatites also serve as sources for exquisite gemstones (Simmons et al., 2003). In the Anti-Atlas, the pegmatites are reported mainly in two lithostratigraphic complexes: (1) in the Paleoproterozoic, associated with the granitic rocks dated around 2 Ga (Morsali et al., 2021 and refences therein). Some of these pegmatites are actively mined for beryl and muscovite, while others are distinguished by the presence of columbite-tantalite and various phosphate species (Permingeat, 1955; Bouladon et al., 1950; Morin, 1952, Morsli et al, 2021, 2022), and, (2) in the Ediacaran series, related to the pluto-volcanic complex of the OG. In the imiter inlier, within the metasedimentary rocks (gresopelites), strike-slip faults and associated dikes ranging from basic to acidic are present. These faults exhibit variable widths and are characterized by the occurrence of aplite and pegmatite bodies. The latter are poorly documented and require more attention to identify and map the hydrothermal alteration zones associated with these pegmatites and aplites.

Remote sensing has become an essential and very effective tool in the efficient and rapid detection and interpretation of hydrothermal alteration associated with mineralization, thus facilitating prospecting and exploration efforts, particularly in remote, inaccessible, and poorly exposed areas (Chen et al., 2019). Various remote sensing techniques have been developed for the detection of hydrothermal alteration, including Principal Component Analysis (PCA), Spectral Angle Mapper, Band Ratios, and Mixture Tuned Matched Filtering. Among these methods, PCA is considered the most significant and widely employed (Soe et al., 2005; Kratt et al., 2010; Zoheir and Emam, 2014; Shabou et al., 2015).

Selecting the appropriate satellite image is a crucial factor in distinguishing and mapping lithological units. The ASTER (Advanced Spaceborne Thermal Emission and Reflection Radiometer) sensor has demonstrated its efficacy in the field of geology (Rajendran et al., 2013; Pour et al., 2015; Ninomiya, 2016), owing to its high spectral resolution in the shortwave infrared (SWIR) range, which allows for accurate detection of the absorption bands of minerals. The objective of the current study is to utilize ASTER imagery to investigate the spectral properties of alteration minerals associated to different geological units especially around the pegmatite and aplites dikes within the imiter inlier of the Anti-Atlas region in Morocco.

Geological framework

Anti Atlas

The Anti-Atlas range is distinguished by the presence of two distinctive tectonic and geomorphological domais that are separated by the Anti-Atlas Major Fault (AAMF; see Fig. 1). The southwestern domain is characterized by a Paleoproterozoic sequence that was formed during the Eburnean orogeny, whereas the northeastern part is composed of a Neoproterozoic sequence that was created during the Panafrican orogeny (Leblanc, 1975; Hassenforder, 1987; Saquaque et al., 1989; Gasquet et al., 2004, 2008; Thomas et al., 2002, 2004; Ennih and Liégeois, 2008).

In the southwestern domain, the paleoproterozoic series, consist of siliciclastic sedimentary sequences, migmatites, gneisses, and plutonic rocks, with ages ranging from 2.2 Ga to 1.75 Ga (Ikenne et al., 1997; Aït Malek et al., 1998; Mortaji et al., 2000; Thomas et al., 2002; Gasquet et al., 2005; Ikenne et al., 2017; Blein et al., 2022). However, further investigations integrating geophysical, geochronological, and geochemical data have revealed the potential extension of the Paleoproterozoic basement beyond the Neoproterozoic terrains, potentially extending towards the South Atlas fault or even beneath the High Atlas, with a thinned crust (Ennih and Liégeois, 2001, 2008; Gasquet et al., 2008). These rocks are overlain by passive margin sedimentary sequences attributed to the Tonian-Cryogenian Taghdout Group, as described by Clauer (1974) and Thomas et al. (2004). Recent geochronological data obtained from mafic dikes in the Igherm and Zenaga inliers have yielded ages of 1.75 Ga and 1.63 Ga, respectively (Ikenne et al., 2016, 2017; AitLahna et al., 2020), indicating that the deposition of the Taghdout Group occurred on a late

Paleoproterozoic to early Mesoproterozoic passive margin, as reported by Ikenne et al. (2017, 2021b). Furthermore, recent geochronological investigations have revealed the presence of Mesoproterozoic mafic igneous rocks in the western inliers of the Anti-Atlas (El Bahat et al., 2013). Geochronological data also indicate that the volcaniclastic deposits of the Tachdamt Formation have an age of 883 Ma, thereby providing a revised estimate for the timing of the subaqueous volcanic eruption in the Anti-Atlas and the initiation of rifting (Bouougri et al., 2020). This revised age contrasts with the previously proposed age of 788 ± 10 Ma by Clauer (1976). The Northeastern domain is formed by Neoproterozoic series. The remnants of a oceanic domain along the Anti-Atlas Major Fault are recognized in the BouAzzer and Siroua windows, where they are represented by Neoproterozoic ophiolite sequences (Hefferan et al., 2014; Triantafyllou et al., 2020). Drawing upon the analogy with the Appalachian belt, Hefferan et al. (2014) proposed a geodynamic evolutionary model consisting of three stages to explain the origin and closure of the oceanic domain between the northern part of the West African Craton and a hypothetical continent. The first stage corresponds to the initial rifting of Rodinia (885-760 Ma), leading to the establishment of the West African Craton's passive margin and oceanic crust. Recent geochronological data obtained from volcaniclastic deposits of the Tachdamt Formation indicate an age of approximately 883 Ma, thereby providing new insights into the timing of rift initiation in the Anti-Atlas (Bouougri et al., 2020). The second stage, known as the Iriri-Tichibanine orogeny (760-700 Ma), is represented by the Tasriwine ophiolitic complex and the Iriri migmatites in the Siroua inlier, as well as the Tichibanine Ben Legrad Formation, Bougmane, and Tazeghzaout complexes in the Bou-Azzer inlier (Samson et al., 2004; Chèvremont et al., 2013;). The third stage, referred to as the Bou-Azzer orogeny (680-640 Ma), is characterized by the emplacement of numerous syn-tectonic calc-alkaline granodioritic to tonalitic intrusions, dated between 675 and 645 Ma (Inglis et al., 2005; Massironi et al., 2007). A garnet Sm–Nd date of 647.2 ± 1.7 Ma was recently determined for the Tasriwine ophiolitic complex in the Siroua inlier (Inglis et al., 2016). The fourth and final stage, known as the West African Craton-Cadomian orogeny (620-555 Ma), was characterized by the development of a high-K continental magmatic arc, followed by the formation of clastic basins represented by the BouSalda, Tiddiline, and Saghro Groups, culminating in collision. The Ediacaran volcanic and volcano-sedimentary rocks of the Ediacaran OG were generated during this episode, corresponding to the Late Neoproterozoic or PIII according to Choubert (1963).

The youngest folded series within the Panafrican inliers, namely the Saghro, BouSalda, and Tiddiline Groups, primarily consist of mafic to intermediate metavolcanic and metasedimentary rocks (Thomas et al., 2004). These units have been assigned either Cryogenian age (Ouguir et al., 1996; Fekkak et al., 2001; Gasquet et al., 2005; Massironi et al., 2008) or Ediacaran age (Liégeois et al., 2006; Abati et al., 2010; Hefferan et al., 2012; Michard et al., 2017). The volcanic series of the Ediacaran OG, accompanied by associated volcanoclastic, sub-volcanic, and plutonic rocks, are widely distributed throughout the majority of the Anti-Atlas region. These volcanic sequences exhibit substantial thicknesses and are characterized by a predominance of andesites, rhyolites, and pyroclastic equivalents (Ikenne et al., 2007; Toummite et al., 2013; Belkacim et al., 2017; Baidada et al., 2017).

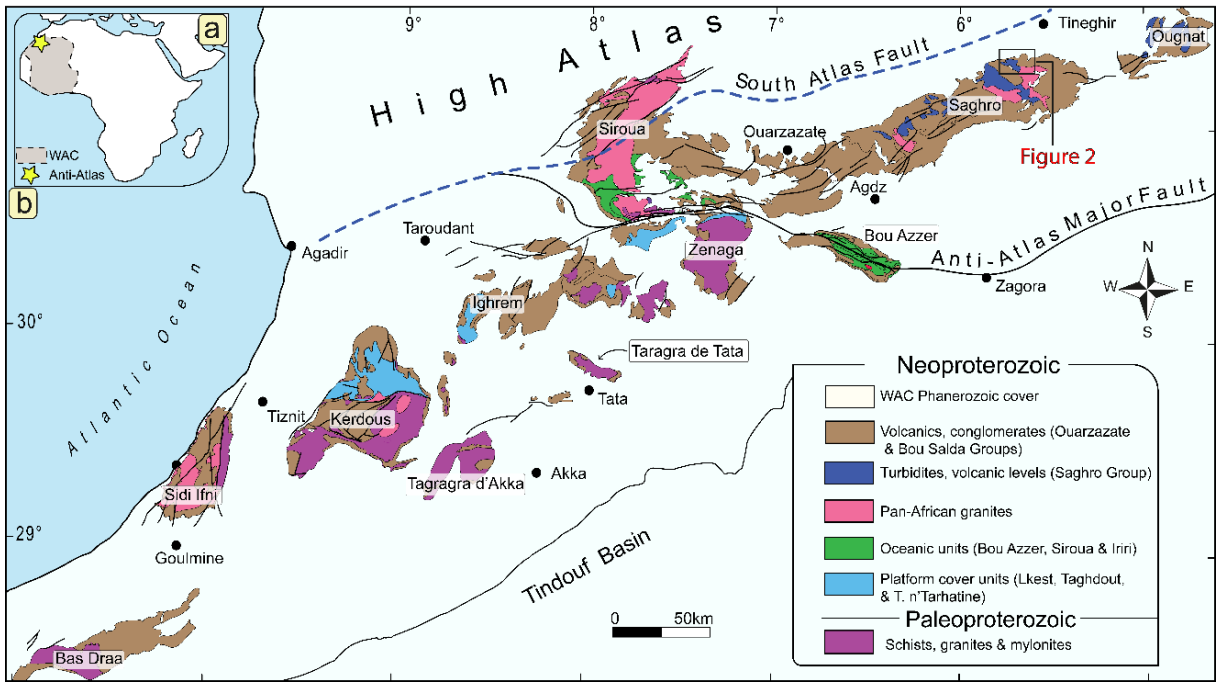

Figure 1:- (a) Simplified map showing the location of the Anti-Atlas belt along the northwestern margin of the WAC. (b) The main Precambrian inliers, including the location of the figure 2 (modified from Gasquet et al., 2005).

Imiter inlier

The Imiter inlier, located in the northern side of the Saghro massif, is composed of an early Ediacaran basement overlain by the late Ediacaran volcaniclastic series of the Ouarzazate Group (Fig. 2). The basement comprises weakly deformed metasedimentary rocks belonging to the Saghro Group, forming a triangular block characterized by turbiditic flysch sediments (Guillou et al., 1988; Leistel and Qadrouci, 1991; Ouguir et al., 1994; Barodi et al., 1998; Baroudi et al., 1999; Cheilletz et al., 2002; Fekkak et al., 2002; Levresse et al., 2004). The unconformably overlying series of the Ouarzazate Group and consists of a thick volcano-sedimentary succession. Various authors have established a detailed stratigraphic column of the strata, including andesitic and rhyolitic lavas, rhyolitic ignimbrites, inter-bedded pyroclastic, epiclastic, and sedimentary rocks (Bajja, 1987; Leistel et al., 1991; Ouguir, 1997; Gasquet et al., 2005). These volcanic units are intruded by a significant swarm of basalts, basaltic andesites, andesites, quartz-microdiorites, keratophyres, aplite, and pegmatite (Ikenne et al., 2007). The Ediacaran granitoids in the Imiter area exhibit geochemical characteristics resembling arc-related magmas (Errami et al., 2009; Baidada et al., 2017). Furthermore, the mafic dikes in the area display volcanic arc geochemical signatures (Ikenne et al., 2007).

The SG, which constitutes the oldest rock formations in the eastern Anti-Atlas belt, extends from the Siroua to the Saghro and Ougnat massifs (Michard et al., 2017). This group primarily consists of metaturbidites that have undergone minor deformation and metamorphism in the greenschist facies, along with mafic to intermediate metavolcanic rocks (Hindermeyer, 1953; Ouguir et al., 1996; Fekkak et al., 2001). These rocks are distributed across various sub-inliers within the Imiter, Boumalne, Qal'atM'gouna, and Sidi Flah areas. The metasedimentary rocks are unconformably overlain by the M'gouna and Ouarzazate Groups (Thomas et al., 2004).

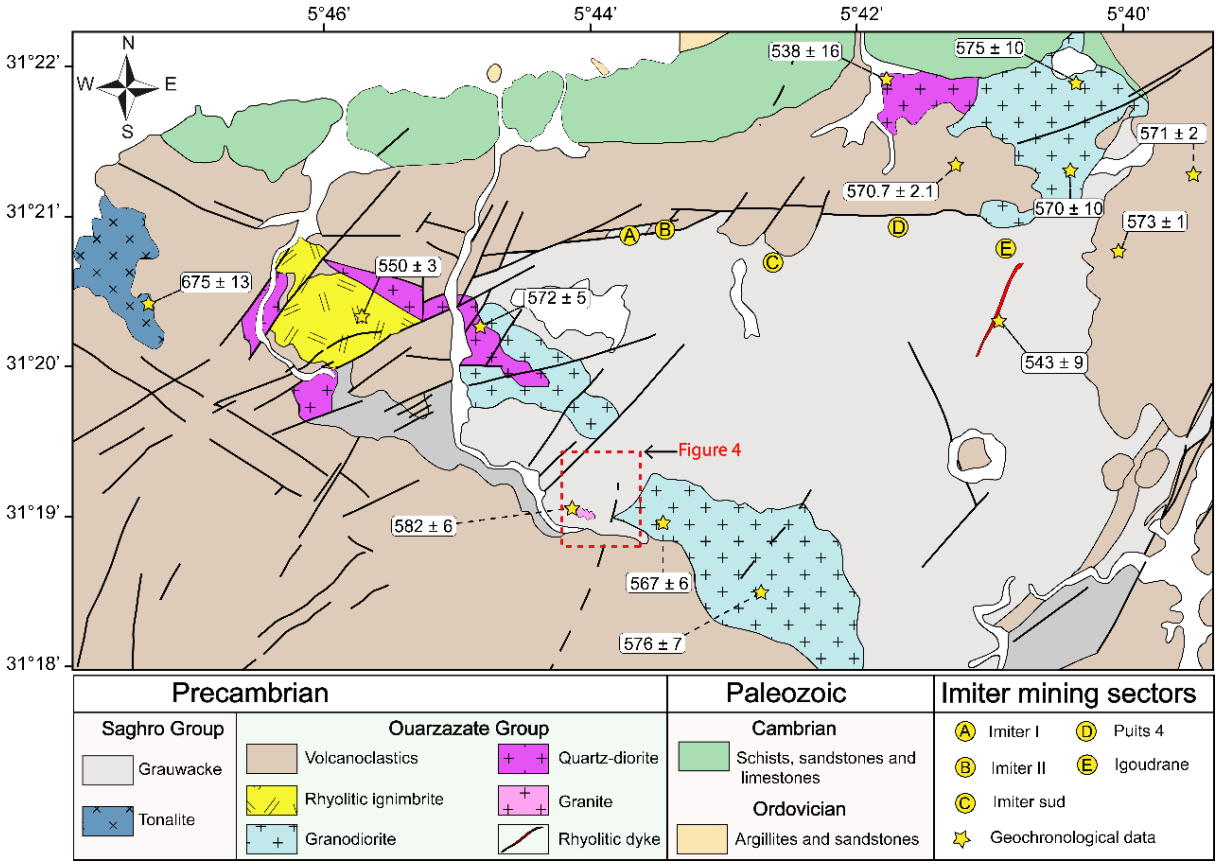

Figure 2:- Geological map of the Imiter inlier showing the locations of the currently exploited mines (modified from Ikenne et al., 2007). See figure 1for the location.

Methodology:-

The methodology used to achieve the objectives outlined in the study is summarized in the flowchart presented in figure 3. Through field observations and petrographic analysis, the constituent minerals of the paragneiss were identified, as well as various alteration types. Furthermore, detailed mapping of the study area was carried out. The methodology involves using the Level 1 ASTER image downloaded from the website www.earthdata.nasa.gov, with an acquisition date of April 1, 2006. The raw image requires pre-processing procedures to correct for geometric and radiometric errors before analyzing and processing the spectral data in ENVI software (Ranjbar 2011; Sadeghi et al., 2013; Alimohammadi et al., 2015; Testa et al., 2018). Geometric correction is performed by converting the raw image into an orthorectified image for more accurate analysis. Radiometric correction is also essential to ensure the quality of data provided by remote sensing sensors (Lowell and Guilbert 1970). However, ASTER data may be affected by the problem of crosstalk, which is an error of offset or additive nature (Rowan and Mars, 2003). Radiance is due to the leakage of photons from one detector element to another, and this is more pronounced from band 4 to bands 5 and 9, but it also affects all SWIR bands. The crosstalk effect will approach 100% of the input radiance signal for very dark pixels adjacent to bright pixels. A spatial software correction for crosstalk was developed by Iwasaki et al. (2001) and has been incorporated by the Moroccan ASTER ground data system (GDS) as part of its Level 1 pre-processing. To map hydrothermal alterations, the "Band Ratio" approach is used. This ratio is calculated by dividing the sum of values of two specific bands by the value of another band. In particular, for argillic alteration, the ratio of the sum of bands 4 and 6 to band 5 is calculated. This band combination is sensitive to clay minerals that strongly absorb in band 6. For phyllic alteration, the ratio of the sum of bands 5 and 7 to band 6 is calculated. This band combination is sensitive to phyllic minerals that have silica and iron absorptions in bands 5 and 7. Finally, for propylitic alteration, the ratio of the sum of bands 7 and 9 to band 8 is calculated. This band combination is sensitive to propylitic minerals rich in chlorite and epidote, which have iron and magnesium absorptions in bands 7 and 9 (Alimohammadi et al., 2015; Zamyad et al., 2019). These ratios enable the detection and mapping of hydrothermal alterations in the study area.

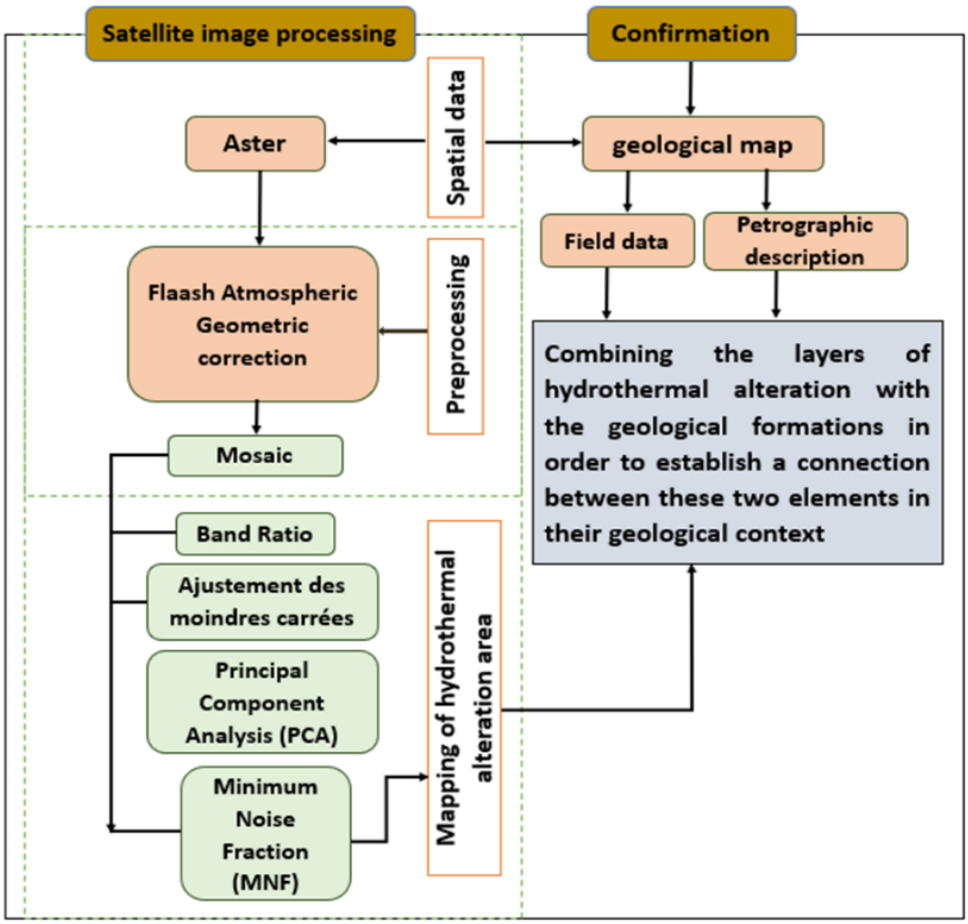

Figure 3:- Diagram of the applied model methodology.

Results:-

ASTER data

The reflectance values in different bands facilitated the computation of different ratiosand allow identifying three distinct types of alteration: argillic, phyllic, and propylitic (Fig. 4a). The prevalence of clay alteration indicates a substantial occurrence of clay minerals, which is strengthening by the elevated ratio of the sum of bands 4 and 6 to band 5. Argillic alteration occurs when primary minerals undergo chemical transformations in the presence of water and oxygen, leading to the formation of clay minerals. The grauwacke units and some volcanoclastic rocks exhibit significant argillic alteration compared to pegmatites, diorites, and granites. This disparity arises due to the latter rocks' composition and texture, which comprise minerals that resist the weathering process (Fig. 4b). Although aplite and pegmatite rocks may exhibit similar levels of argillic weathering due to their mineral resilience, the specific mineralogical composition of rocks in the study area may result in varying degrees of weathering. To identify phyllic minerals, the ratio between the sum of reflectance values in bands 5 and 7 and band 6 is computed, as these bands capture the absorption of silica and iron by phyllic minerals (Fig. 4c). Phyllitic alteration offers valuable insights into the origin and nature of associated mineralization in various rock types, including grauwacks of the Saghro Group, aplite, pegmatite, and select volcanoclastic rocks within the Imiter mine's triangular region. This alteration is also observed along major faults within the study area. The spatial distribution of this alteration is nearly identical to the previously mentioned argillic alteration.

Propylitic weathering is assessed by calculating the ratio between the sum of reflectance values in bands 7 and 9 and band 8, which is sensitive to propylitic minerals exhibiting absorption in bands 7 and 9 (refer to Fig. 4d; Alimohammadi et al., 2015). This type of alteration is commonly observed in the volcanoclastic and plutonic rocks of the OG, as well as along major faults. The prevalence of volcaniclastic and plutonic rocks in the area contributes to the presence of propylitic minerals such as epidote, chlorite, and calcite, which are characteristic outcomes of

propylitic alteration. Interestingly, it is noteworthy that this alteration is entirely absent in the volcanoclastic rocks of the OG.

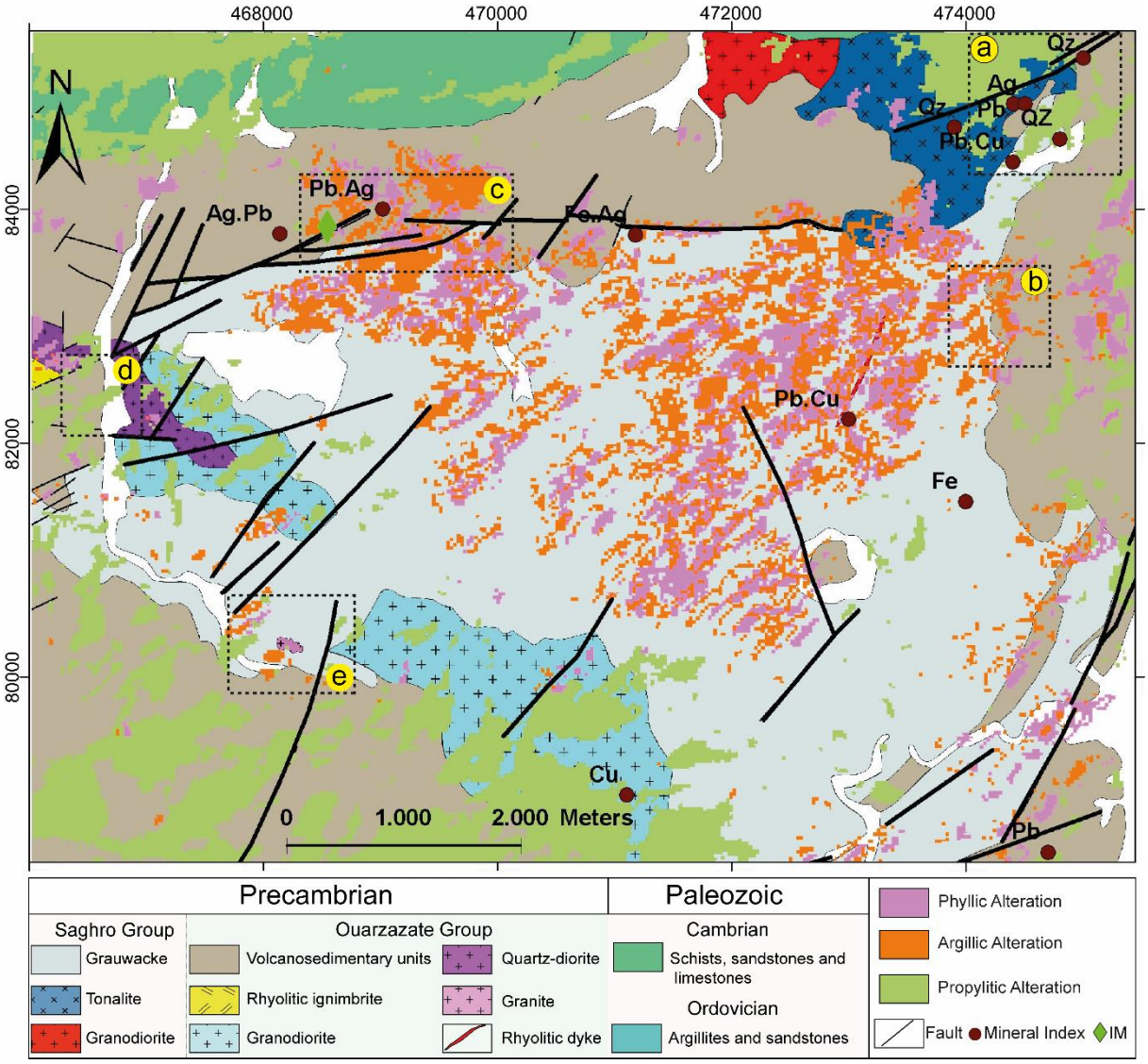

Figure 4:- Mineral map showing the results of the matched filtering method using ASTER data overlaid on the ASTER image. (a) Clay, phyllic and propylitic alterations. (b) Clay alteration. (c) Phyllic alteration. (d) Propylitic alteration.

Field data and petrography

Aplite dikes

The studied samples of aplite were collected from several veins trending NE-SW and NW-SE (Fig. 5). These veins have variable thickness ranging from 1 m to 3 m, but they can reach up to 10 m (Fig. 6a and 6d). They intrude the lower Ediacaran metasedimentary grauwacke with sharp contacts (Fig. 6b, 6c and 6e). The aplite veins exhibit a zoned structure, with large crystals in the center, fine-grained minerals and aplitic texture at the edges, and in some places, large muscovite crystals and quartz patches are observed. Two groups of veins are identified; the first group corresponds to veins with pinkish potassium feldspar dominance, which have undergone intense alteration, while the second group corresponds to veins with whitish alkali feldspar dominance and less alteration. The kaolinization and sericitization of alkali feldspar and plagioclase, respectively, are weak.

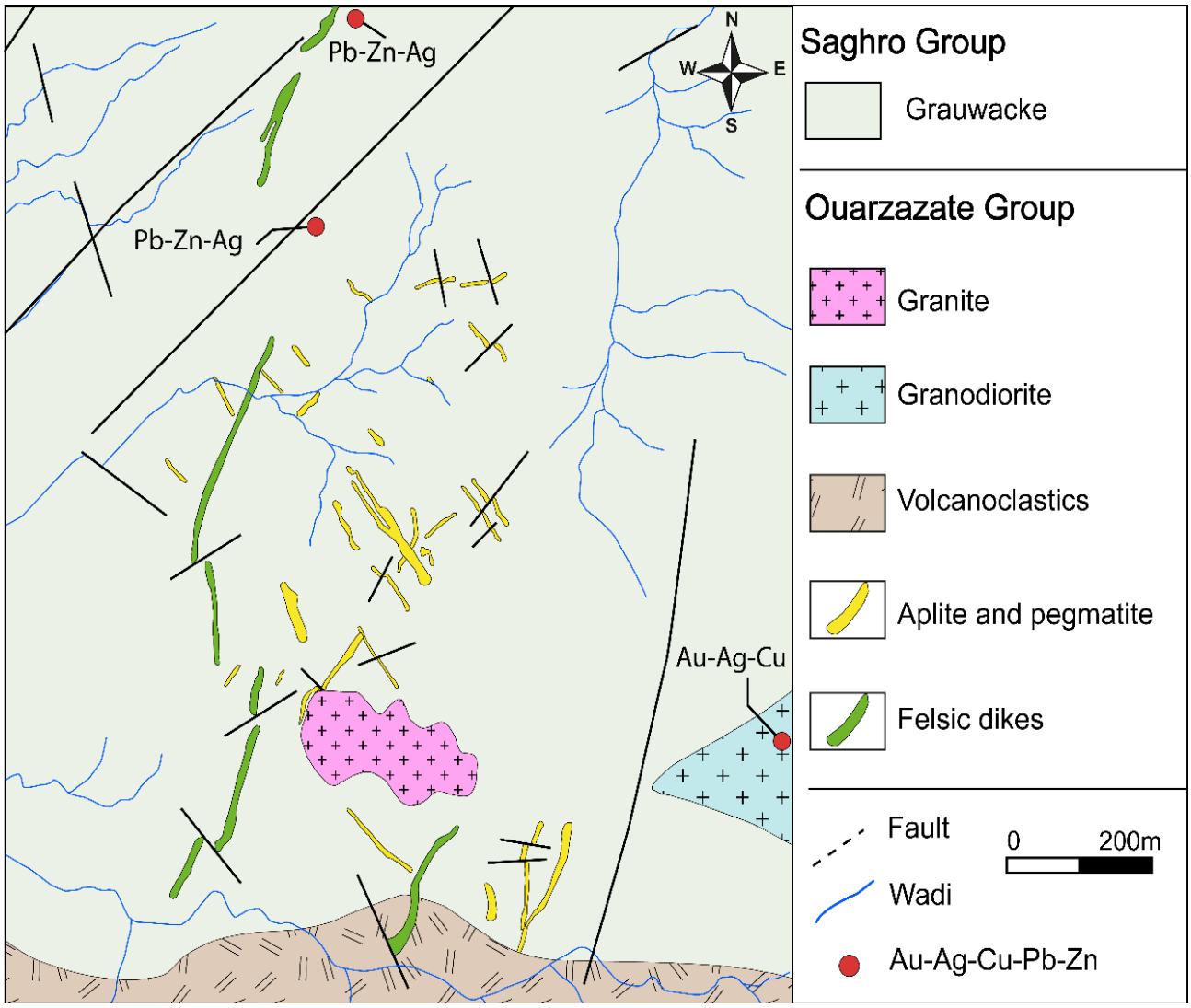

Figure 5:- Detailed geological map of the zone containing the aplite and pegmatite dikes is depicted in figure 3, indicating their location.

The rock exhibits a holocrystalline appearance with a granular texture. Microscopic observations revealed that these aplites are composed of a primary paragenesis of feldspar, quartz, muscovite, and opaque minerals (Fig. 7a and 7b), as well as a secondary paragenesis of sericite and clay minerals. Although these rocks exhibit the same mineralogical paragenesis, some specific aspects of each sample can be illustrated. The observed alkaline feldspars are orthoclase and microcline, appearing as small xenomorphic crystals measuring between 0.5 and 0.75 mm, with microcline being dominant (Fig. 7f). In some samples, orthoclase dominates, ranging in size from almost 3 to 4 mm, with microcline measuring 2 to 3.5 mm. Microcline is dominant in some samples and is of a larger size. As for orthoclase, it appears as xenomorphic to subautomorphic with a size of approximately 1.25 mm. Plagioclase is present in low amounts, generally subautomorphic in shape, with a size of several mm and averaging 2.5 mm. Inclusions of metallic oxides (Fig. 7c and 7d) are often observed within the feldspars. Like the feldspar, the quartz does not always appear the same shape. It occurs either as xenomorphic to subhedral crystals with an average size of 0.25 to 1.5 mm or like crystals of 2.5 mm in size, in a intergrowths association with the alkali feldspars forming a graphic texture. At times, the crystals can reach 3 to 4 mm in size, xenomorphic but occasionally appearing as droplets in the alkali feldspars to create a myrmekitic texture in places (Fig. 7e). Muscovite is slightly abundant and is observed as subhedral microcrystals (Fig. 7a).

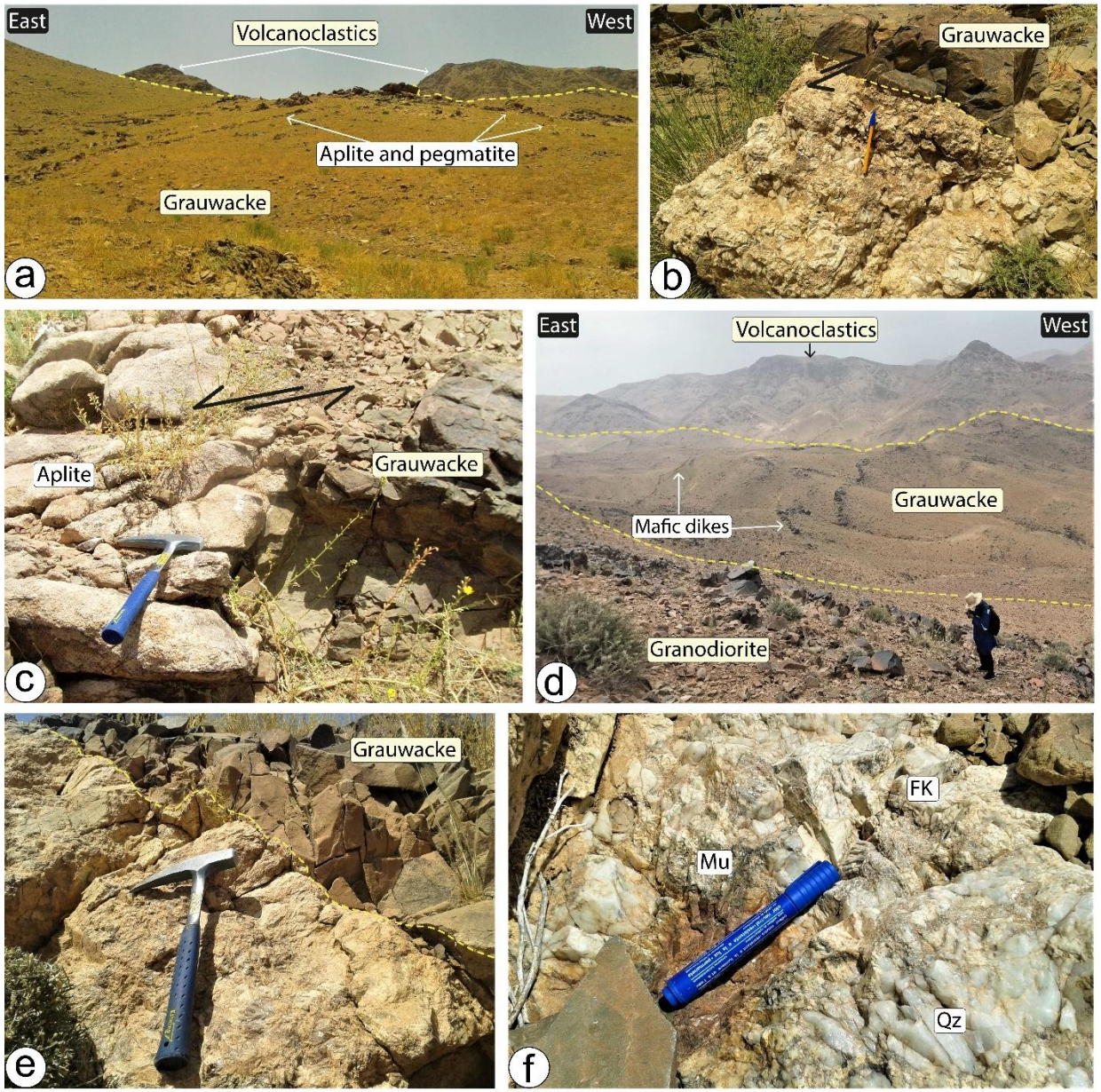

Figure 6:- Microphotographs depicting the mineral paragenesis of the Bou Teglimt aplite and pegmatite dikes are shown in figure 3. (a) illustrates the aplite and pegmatite dikes in two directions NE-SW and NW-SE, while (b) and (c) show the pegmatite and aplite dikes, respectively, in contact with grésopelites. (d) provides a panoramic view of the acidic and basic dikes enclosed within the grésopelites (view towards the south). In (e), a pegmatite dike is shown in contact with grésopelites, displaying a zonation from the periphery to the center. (d) Depicts large crystals of feldspar (FK), muscovite (Mu), and quartz (Qz) in a pegmatite dike.

Pegmatite dikes

The BouTeglimt pegmatitic dikes exhibit distinct boundaries with the surrounding host rocks, displaying internal zoning characterized by intricate mineralogy and textures, and occasionally containing xenoliths derived from the host rocks. The intermediate zones within these pegmatitic dikes primarily consist of quartz, magnetite, and feldspars, with minor occurrences of allanite and sphene. Aplite lenses, reaching lengths of up to 200 m and widths of 15 m, are found along the sinistral NW-SE strike-slip fault and its associated shear zones. The BouTeglimt pegmatites occur as veins about 3m in thickness, they are composed of feldspar, quartz and abundant muscovite (Fig. 6f). The primary and secondary parageneses are almost identical to those observed in the previously described aplite veins. The feldspars remain dominant, with microcline being the most abundant variety and occurring as

phenocrysts. Plagioclase occurs sporadically in small, subautomorphic crystals. The second most abundant mineral is quartz, which is present as decimeter-sized, xenomorphic to subautomorphic phenocrysts. Quartz crystallizes in the form of writing included in alkali feldspar, with the same optical orientation, to locally create a graphic texture in the rock. In addition to feldspars and quartz, muscovite occurs in the form of elongated, subautomorphic crystals. Allanite and titanite, as well as opaque minerals, occur in small crystals as inclusions in other minerals.

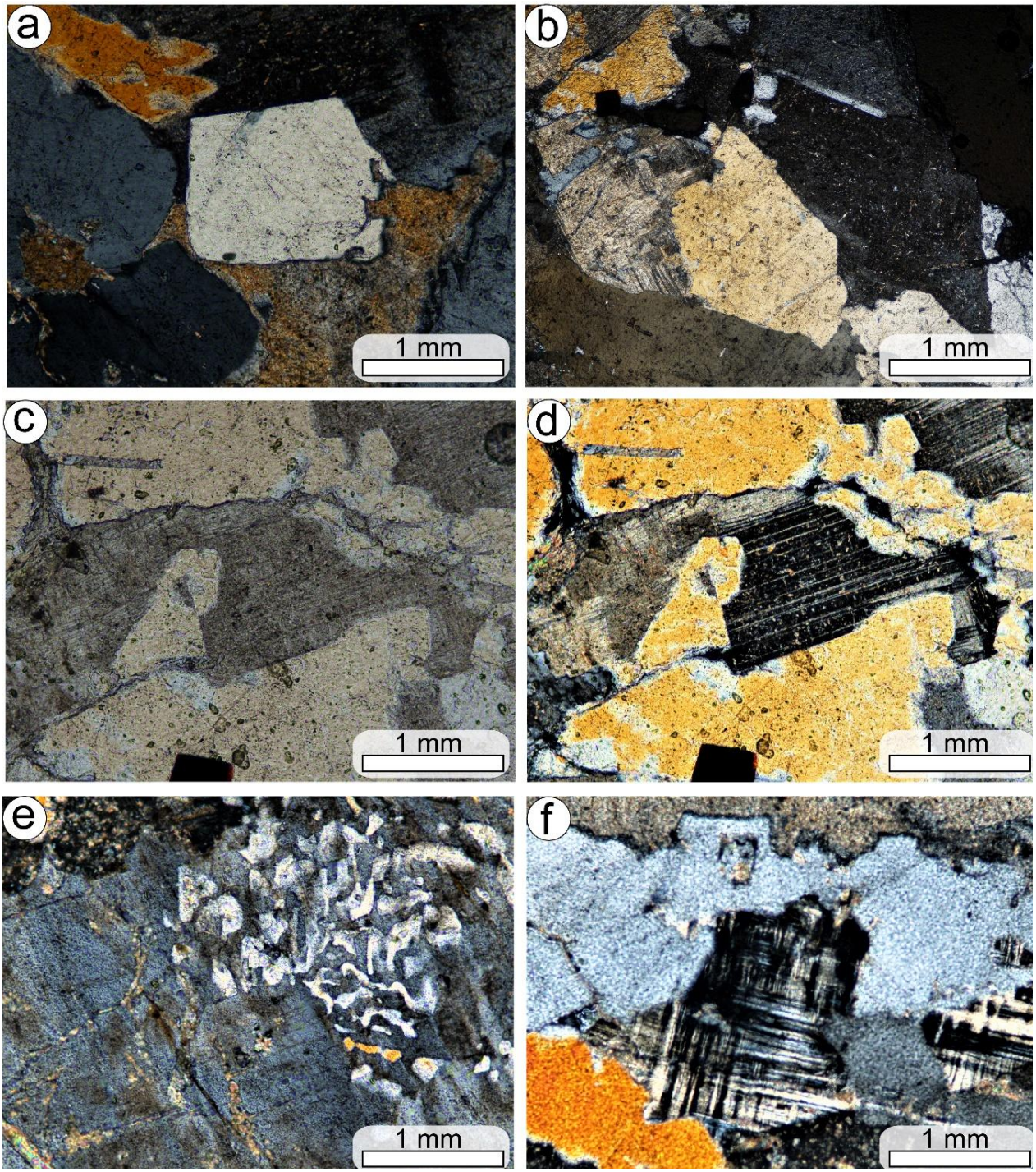

Figure 7:- Microscopic photographs are presented to illustrate the mineral paragenesis observed in the Bou Teglimt aplite and pegmatite dikes (see text for details).

Discussion:-

Zoning of Pegmatitic and Aplitic veins

The prevailing model for the formation of pegmatitic melts is attributed to the process of fractional crystallization within a granitic pluton (Jahns & Burnham, 1969). During progressive fractionation, the composition of the fertile granite undergoes changes, starting from biotite granite at greater depths, transitioning to two-mica leucogranite, coarse-grained muscovite leucogranite, and eventually to pegmatitic leucogranite. This pegmatitic leucogranite is characterized by intercalated layers of sodic aplite and potassic pegmatite near the roof of the intrusion (Černý and Meintzer, 1988; Černý, 1989). It is uncommon to find the complete sequence exposed within a single intrusion due to erosion levels determining the number of rock types visible on the surface. In the case of the Imiter inlier, the BouTeglimt granodiorite, a late Pan-African intrusion (567 ± 6 Ma; Baidada et al., 2018), is located along the southwestern side of the Imiter silver deposit. The BouTeglimt intrusion takes the form of an elongated body oriented in the NW-SE direction, covering an approximate area of 3.5 × 1.5km (see Fig. 2). BouTeglimt pegmatite and aplite are observed in clusters or swarms within weakly metamorphosed sandstones and black shales, suggesting a probable derivation from large plutons of granitic and granodioritic composition. Three groups of pegmatites have been identified based on their proximity to the related pluton: interior, marginal, and exterior pegmatites (Černý, 1991). The BouTeglimt pegmatite and aplite are classified as exterior pegmatites, situated outside the pluton within the metamorphic country rocks.

The BouTeglimt aplitic and pegmatitic dikes exhibit distinct boundaries with the surrounding host rocks, displaying internal zoning characterized by intricate mineralogy and textures. The intermediate zones within these pegmatitic dikes primarily consist of quartz, magnetite, and feldspars, with minor occurrences of allanite and sphene. The aplite lenses possess a zoned complex structure, exhibiting the same mineral composition as the pegmatitic dikes. Zoning within pegmatites can be observed at two scales: (i) internal zoning, denoting mineralogical and textural variations within individual pegmatite bodies, and (ii) regional zoning, which manifests as an increase in mineralogical complexity with distance from the granitic source. According to Černý (1991), the zonation is influenced by the nature and structure of the host rock. The distribution pattern of rare elements within the zoned pegmatites follows the sequence: a) barren to Be-rich; b) Be-Nb rich; c) Li-Cs-Ta-Sn-rich (Černý, 1991; Fig. 8).

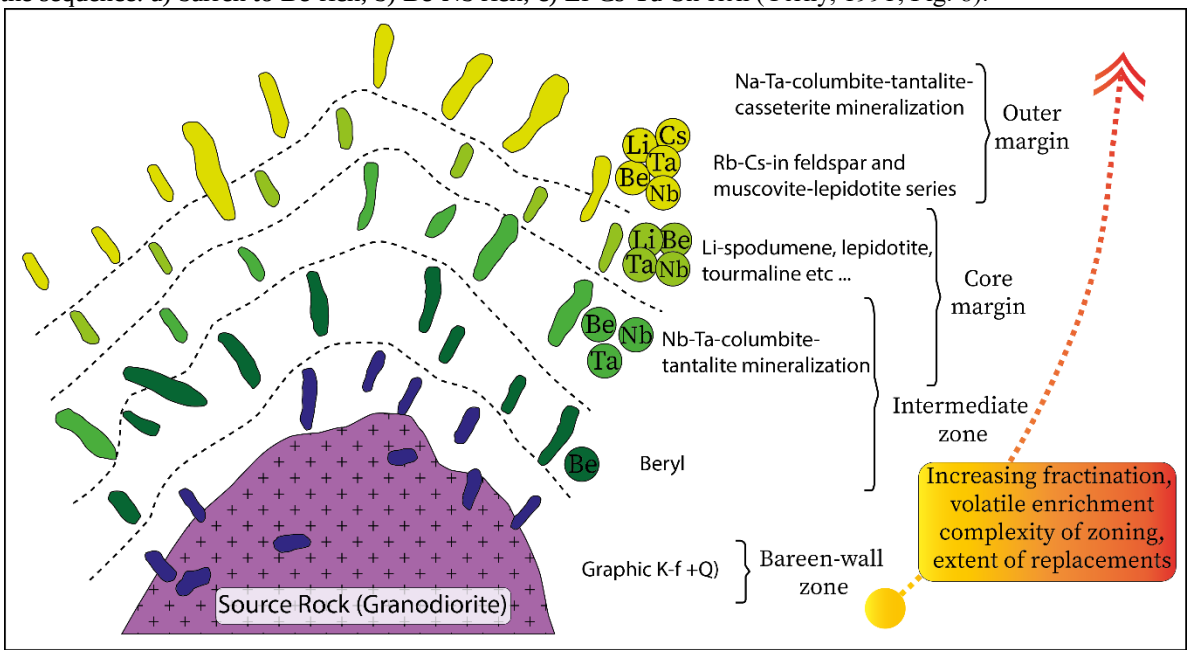

Figure 8:- Shematic evolution and regional zoning in a cogenitic parent granite and pegmatite group (modified from Černý, 1991and London, 2016) . The shematic representation show a pegmatite increase in degree of evolution with increasing distance from the parent source rock.

Pegmatite and aplites:exploration prospects

Within the Early Ediacaran grauwackes located south of the Imiter Ag deposit, there are numerous pegmatite and aplite dikes that have received limited investigation regarding their mineral paragenesis and their relationship with hydrothermal ore mineralization. Based on their mineralogy and morphology, the BouTeglimtaplites and pegmatites

exhibit a granitic composition rich in muscovite, with a dominance of orthoclase, microcline, and quartz. Evidence of magmatic mineralization is attested by the presence of thorite and zircon, while hydrothermal activity is indicated by the alteration of feldspars and the formation of pyrite and iron oxides, potentially associated with radioactive minerals. Moreover, Baidada et al. (2017) have highlighted the presence of BouFliou sulfide-magnetite mineralization in the northwestern part of the BouTeglimt granodiorite intrusion. Silicification and potassic alteration are associated with veins, stockworks, and breccias rich in iron oxides (> 10 vol %), occurring along NE-SW faults. Interestingly, these structures share the same orientation as the majority of the aplitic and pegmatitic veins.

Pegmatites exhibit variations in their mineralogical composition, which can be classified as either homogeneous or heterogeneous. Homogeneous pegmatites, although not widely valuable, can hold significance in certain cases where they are exploited for lithium, feldspar, or micas (Guilbert and Park, 1986). The BouTeglimt pegmatites and aplites, on the other hand, are characterized by their abundance of muscovite. Muscovite serves as an excellent exploration indicator as it occurs in both fertile granites and rare-element pegmatites, and is particularly useful in identifying potential tantalum (Ta) mineralization (Černý, 1989a; Morteani and Gaupp, 1989). Tantalum and niobium have a strong affinity for muscovite and tend to preferentially partition into titanium-bearing minerals, such as rutile and titanite (Linnen and Cuney, 2005). Consequently, the tantalum content of muscovite has been employed as an exploration tool, with pegmatites containing muscovite exhibiting Ta concentrations greater than approximately 80 ppm considered to hold economic potential for tantalum (Černý, 1989).

The epidote-group minerals exhibit considerable variability in their compositions and stability across a broad range of temperatures and pressures, making them significant components of various igneous, metamorphic, and hydrothermal rocks (Franz and Liebscher, 2004). However, epidote is not commonly found in pegmatites, occurring only sporadically as an accessory mineral (Dill, 2015; Palinkaš et al., 2012; Wise, 2019). The formation of rock assemblages containing epidote-bearing minerals necessitates elevated calcium (Ca) levels, low phosphorus (P) and fluorine (F) contents, and high oxygen fugacity (fO_2) conditions (Wise, 2019). The presence of abundant allanite within the BouTeglimt pegmatites implies a certain degree of economic potential, as reported in certain granite pegmatites (Mariano, 1989). The occurrence of allanite and apatite in subsequent mineralization phases indicates the mobilization of light rare earth elements (LREEs) from titanite (also observed by Pan et al., 1993a. Mazdab et al. (2007) noted the wide compositional diversity of titanite in hydrothermal environments. The original magmatic REEs can be remobilized through hydrothermal and metasomatic processes (e.g., Oliver et al., 1999; Wang and Williams, 2001). Magmatic fluids can contain relatively high concentrations of LREEs (e.g., Pan et al., 1993b; Kwak and Abeysinghe, 1987).

Hydrothermal alteration

In the discussed imiter inlier area, the grauwacke, aplite, and pegmatite formations commonly exhibit clayey, phyllitic, and propylitic alterations, particularly in the contact zone between the SG and OG in the southern vicinity of the Imiter mine. The grauwackes within the SG display two notable types of alteration, namely phyllitic and argillic alterations. Previous studies (Levresse et al., 2004; Ikenne et al., 2007; Essarraj et al., 2016) have established a connection between these alteration patterns and indicators of mineralization, including lead sulfides, iron oxides, and potentially silver ore deposits. To support these findings, the observed alteration patterns have been geologically mapped and subsequently validated in the field. This approach has led to the identification of new zones within the study area that exhibit promising metallogenic potential, as illustrated in figure 9.

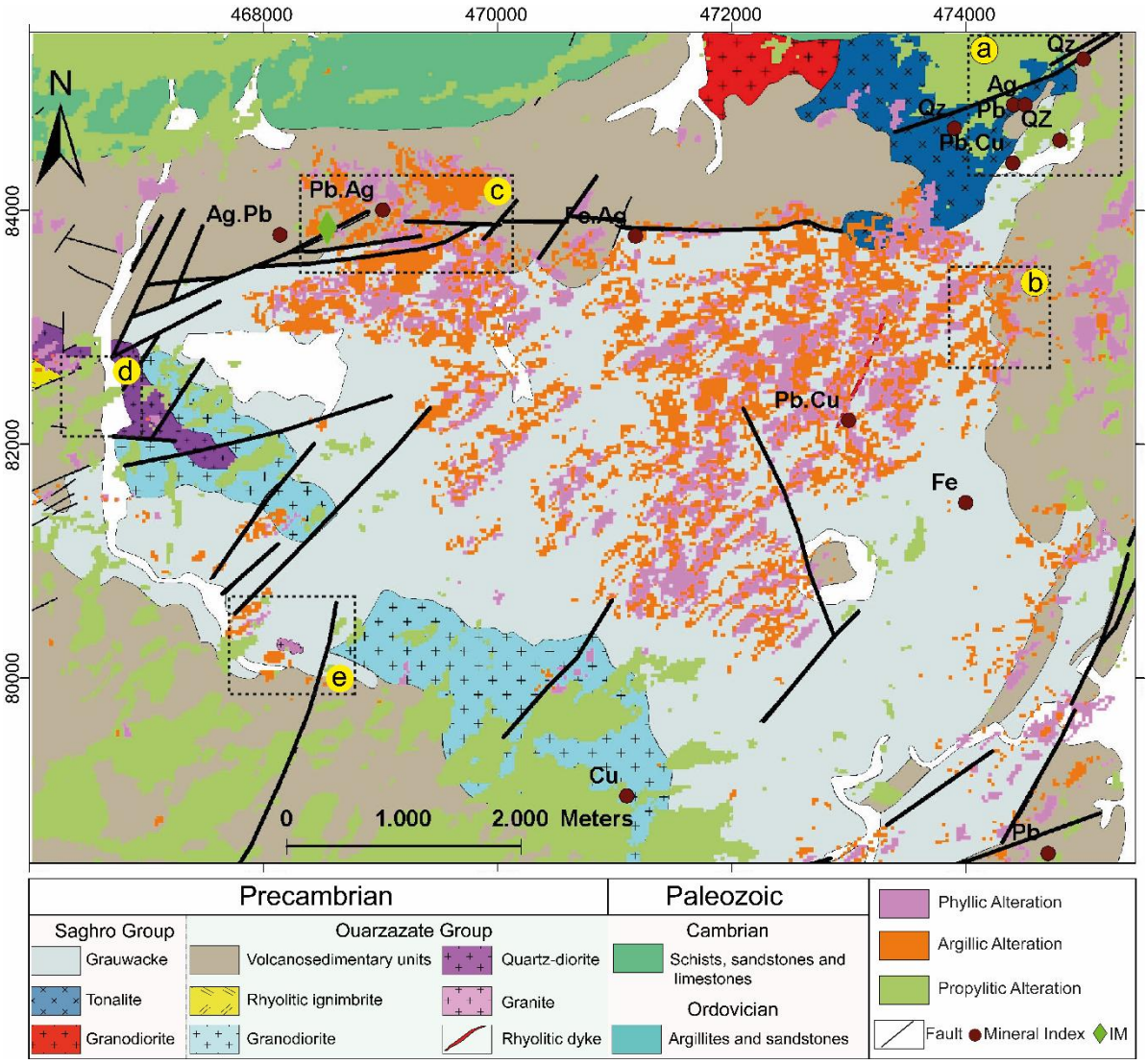

Figure 9:- Interpreted alteration map overlaid on the geological map showing the location of sampled field sites with an economic potential.

The presence of altered clays can serve as an indication of the existence of hydrothermal minerals like montmorillonite or kaolinite. In the study area, the grauwacke units and certain volcanoclastic rocks exhibit a pronounced occurrence of argillic alteration in comparison to pegmatites, diorites, and granites. This difference can be attributed to the compositional and textural characteristics of the latter rock types, which make them more resistant to alteration (Fig 9, 10, and 11). The observed argillic alteration occurs in the form of NE-SW-oriented bands, parallel to the layering of strata and various associated basic dikes. Furthermore, this alteration is also localized at the contact zone between the OG detrital rocks and volcanic rocks. Within these contact zones, the presence of quartz veins filled with sulfides and oxides has been confirmed (Fig 10a). This alteration is described in thin sections and may serve as an indicator of lithium-rich minerals within the pegmatites and aplite formations of BouTeglimt. Similarly, in aplite formations, clay alteration can signify the presence of hydrothermal minerals such as copper, lead, or zinc sulfides, which are frequently associated with aplites (Fig 10-b).

Phyllitic alteration is a prominent feature observed in geological environments that are enriched with acidic hydrothermal fluids, including magmatic intrusions (Fig 10c) and fault zones (Fig 10a, 10d, 11a and 11d; Alimohammadi et al., 2015). In the study area, rocks undergoing phyllitic alteration display a layered or schistose appearance, characterized by easily decomposable layers. Similar to argillic alteration, the presence of phyllitic minerals can serve as a reliable indicator of zones with potential for precious metal-rich mineralization, such as gold

and silver. These minerals exhibit an affinity for acidic hydrothermal fluids, which contribute to the development of phyllitic alteration (Diallo et al., 2022; Alirezaei and Mohammadzadeh, 2009). Within the aplite and pegmatite environment near the Imiter mine, the occurrence of phyllitic alteration may indicate the presence of a zone with potential for precious metal mineralization, including sulfides, silver, and gold (Baidada et al., 2017 and references therein). These metals are known to have a preference for acidic hydrothermal fluids, often associated with phyllitic alteration. Additionally, the presence of phyllitic minerals such as chlorite can be indicative of the occurrence of sulfides like pyrite, chalcopyrite, and galena, which are commonly associated with silver mineralization (Fig 11c; Levresse et al., 2016 and references therein).

Propylitic alteration is a commonly observed phenomenon in the study area, particularly in volcanoclastic, aplite, pegmatite, and plutonic rocks, which are frequently associated with base metal mineralizations such as copper, lead, and zinc (Fig 11b, 11c, and 11e). This type of alteration typically occurs under conditions of elevated temperatures and in the presence of acidic fluids, including sulfur dioxide and hydrogen chloride. The presence of epidote often serves as an indicator of copper and zinc mineralizations, while chlorite may suggest the presence of copper and iron sulfides (Fig 11c, 11d). It is important to note, however, that the occurrence of propylitic alteration does not guarantee the presence of base metal deposits (Liu et al., 2023).

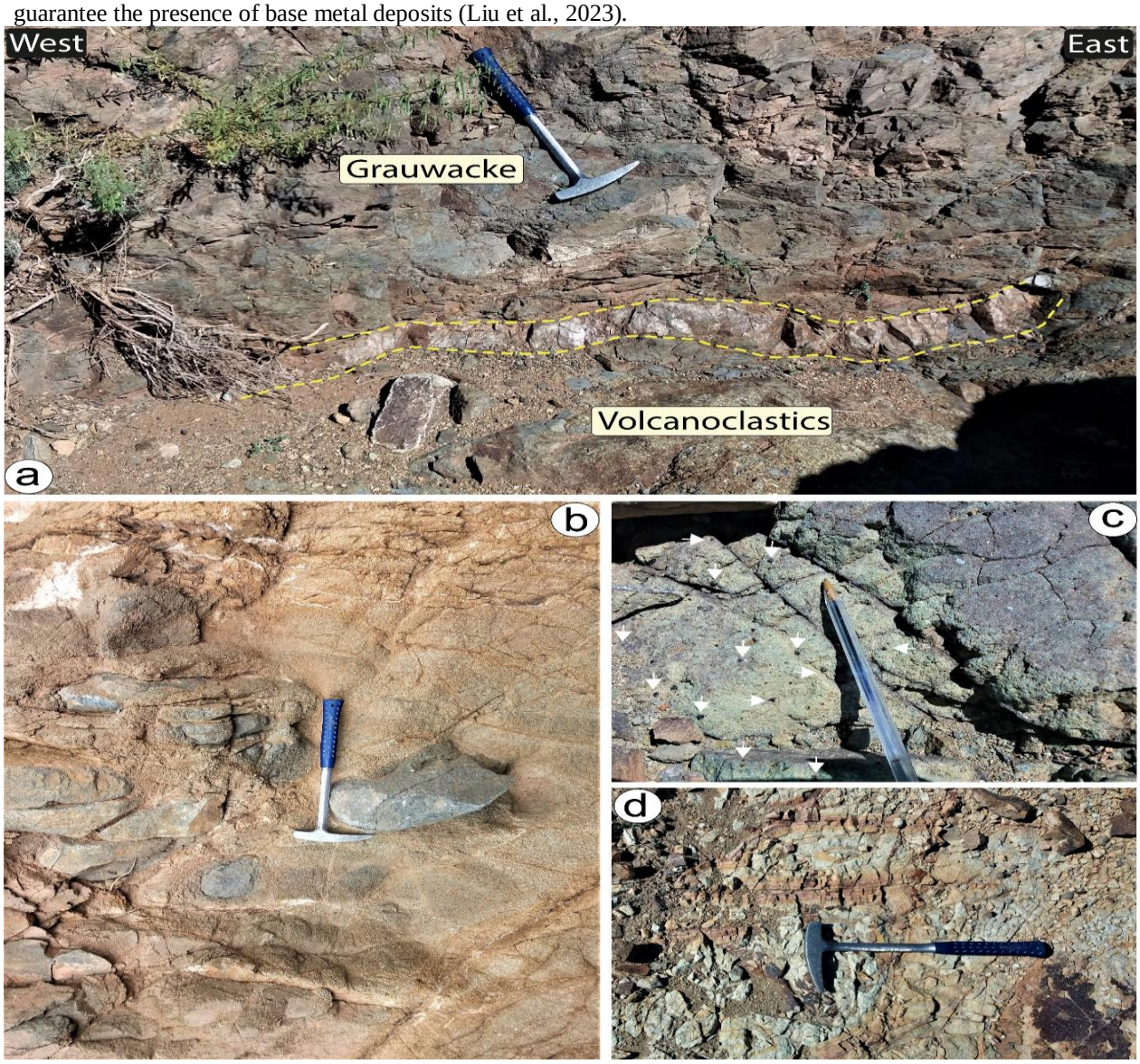

Figure 10:- (a) Faulted contact between SG grauwackes and pyroclastic rocks at the base, filled with and crossed by a mineralized quartz vein. (b) Granodiorite rock showing strong hydrothermal alteration. (c) Altered pyroclastic rock containing millimeter-sized sulfur-bearing minerals. (d) Fine greenish tuffs showing strong hydrothermal alteration.

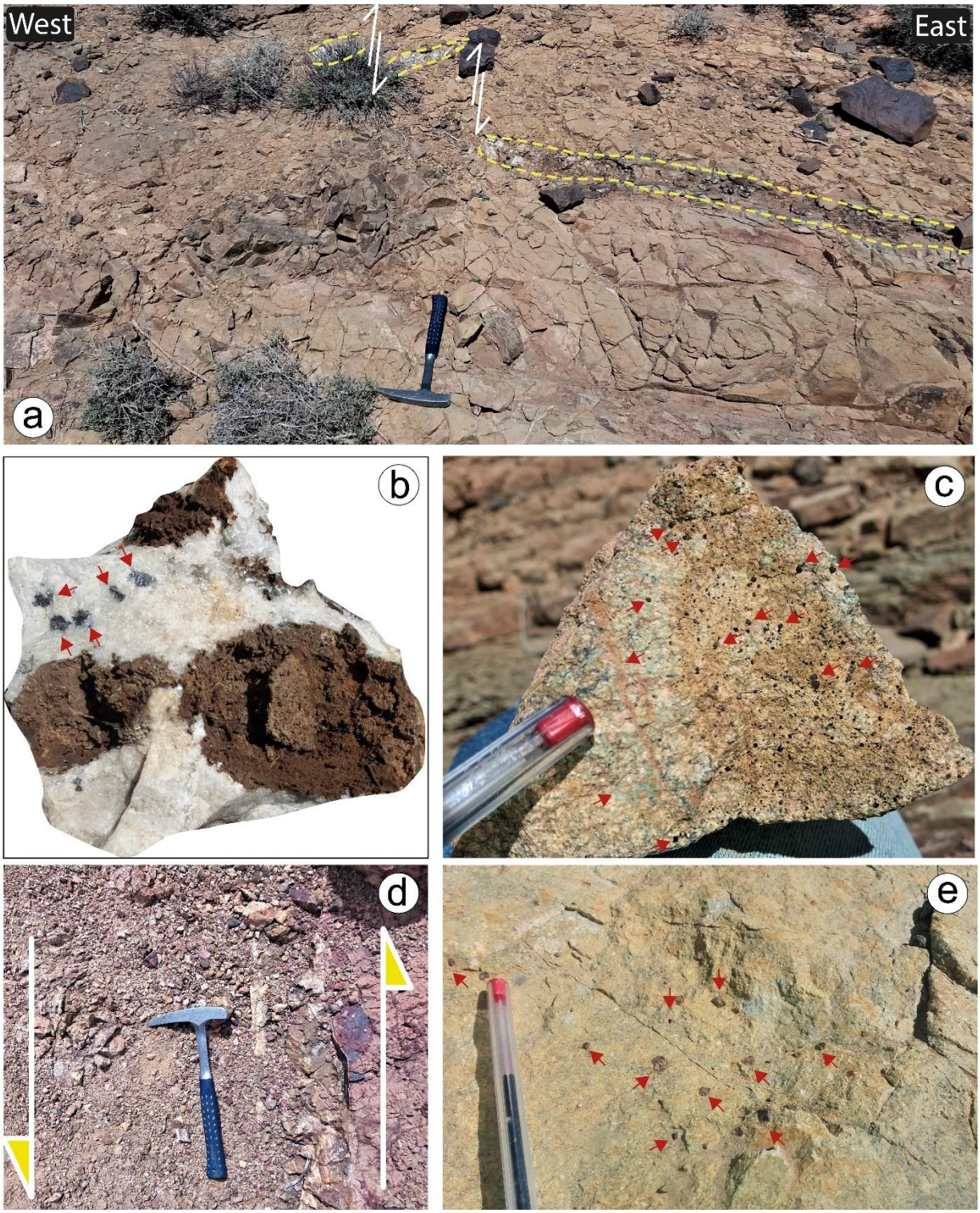

Figure 11:- (a) Highly fractured and altered pyroclastic rock intersected by quartz veins containing sulfides and oxides. (b) Freshly broken sample exhibiting galena and pyrite minerals enclosed in a quartz gangue. (c) Sample of tuffaceous pyroclastic rock containing millimeter-sized oxidized pyrite minerals. (d) Mineralized structure containing sulfides and iron oxides enclosed in a quartz gangue. (e) Outcrop of volcanoclastic rock containing large-sized pyrite minerals.

Conclusion:-

This study utilized the ASTER sensor to investigate significant clayey, phyllitic, and propylitic alterations in the pegmatites and associated rocks (grauwacke, volcaniclastics, aplite) within the Imiter mine area. The aplitic and pegmatitic dikes at BouTeglimt display well-defined boundaries with the host rocks, exhibiting internal zoning characterized by complex mineralogy and textures. The presence of high muscovite content in these dikes makes muscovite a valuable exploration tool, indicating potential tantalum mineralization. Based on mineralogical and morphological characteristics, the aplites and pegmatites exhibit a granitic nature, dominated by feldspars (orthoclase and microcline), quartz, and muscovite. Clay minerals such as montmorillonite or kaolinite observed in the pegmatites suggest the potential presence of lithium-rich minerals. Moreover, alterations observed in the aplite formations may indicate the occurrence of copper, lead, or zinc sulfides. Validation of these alterations in the field has confirmed the presence of Cu-Ag-Pb-Zn and IOGC mineralization. These alteration patterns serve as essential tools in mining exploration and should guide future exploration and mining activities. Geological mapping and field validation of the observed alteration patterns have led to the identification of new zones within the study area that exhibit promising metallogenic potential. However, it is important to note that further geological investigations, including field analyses, mineralogical examinations, and geochemical analyses, are required to confirm the presence of base metal mineralizations and evaluate their economic viability.

References:-

1. Abati, J., Aghzer, A. M., Gerdes, A., Ennih, N. (2010). Detrital zircon ages of Neoproterozoic sequences of the Moroccan Anti-Atlas belt. Precambrian Research. 181(1-4), 115-128. https://doi.org/10.1016/j.precamres.2010.05.018.
2. AitLahna, A., Youbi, N., Tassinari, C. C. G., Basei, M. A. S., Ernst, R. E., Chaib, L., Barzouk, A., Mata, J., Gärtner, A., Admou, H., Boumehdi, M. A., Söderlund, U., Bensalah, M. K., Bodinier, J. L., Maacha, L., Bekker, A. (2020). Revised stratigraphic framework for the lower Anti-Atlas supergroup based on U–Pb geochronology of magmatic and detrital zircons (Zenaga and BouAzzer-El Graara inliers, Anti-Atlas Belt, Morocco). Journal of African Earth Sciences. 171, 103946. https://doi.org/10.1016/j.jafrearsci.2020.103946.
3. Ait Malek, A., Gasquet, D., Bertrand, J. M., Leterrier, J. (1998). Géochronologie U-Pb sur zircon de granitoïdes éburnéens et panafricains dans les boutonnières protérozoïques d'Igherm, du Kerdous et du Bas Drâa (Anti-Atlas occidental, Maroc). Comptes Rendus de l'Académie des Sciences-Series IIA-Earth and Planetary Science. 327(12), 819-826. https://doi.org/10.1016/S1251-8050(99)80056-1.
4. Alimohammadi, M., Alirezaei, S., &Kontak, D. J. (2015). Application of ASTER data for exploration of porphyry copper deposits: A case study of Daraloo–Sarmeshk area, southern part of the Kerman copper belt, Iran. Ore Geology Reviews, 70, 290-304.
5. Alirezaei, S., &Mohammadzadeh, Z. (2009). Hydrothermal alteration-mineralization at Chahfiroozeh porphyry copper deposit, Kerman province, southern Iran. Geological Association of Canada-Mineralogical Association of Canada-American Geophysical Union Joint Assembly, Toronto, Abstract GA71A-15.
6. Baidada, B., Cousens, B., Alansari, A., Soulaimani, A., Barbey, P., Ilmen, S., Ikenne, M. (2017). Geochemistry and Sm–Nd isotopic composition of the Imiter Pan-African granitoids (Saghro massif, eastern Anti-Atlas, Morocco): geotectonic implications. Journal of African Earth Sciences. 127, 99-112. https://doi.org/10.1016/j.jafrearsci.2016.08.016.
7. Baidada, B., Ikenne, M., Barbey, P., Soulaimani, A., Cousens, B., Haissen, F., Ilmen, Said, Alansari, A. (2019). SHRIMP U–Pb zircon geochronology of the granitoids of the Imiter Inlier: constraints on the Pan-African events in the Saghro massif, Anti-Atlas (Morocco). Journal of African Earth Sciences. 150, 799-810. https://doi.org/10.1016/j.jafrearsci.2018.10.008.
8. Bajja, A. (1987). Nouvelles données pétrographiques et géochimiques sur les formations volcaniques précambriennes du JbelSaghro (Anti-Atlas marocain), basaltes en coussin du PII et volcanites de la série d'Ouarzazate (P.III). PhD thesis. Université de Nancy I, France, 225 p. https://doi:10.1127/zdgg/149/1998/1.
9. Barodi, E. B., Belkasmi, A., Bouchta, R., Qadrouci, A. (1998). Les minéralisations argentifères du Maroc : cas du gisement d'Imiter. Chronique de la recherche minière. (531-532), 77-92.
10. Baroudi, Z., Beraaouz, E. H., Rahimi, A., Saquaque, A., Chouhaidi, M. Y. (1999). Minéralisations polymétalliques argentifères d'Imiter (JeblSaghro, Anti-Atlas, Maroc) : minéralogie, évolution des fluides minéralisateurs et mécanismes de dépôt. Chronique de la recherche minière. (536-537), 91-111.
11. Belkacim, S., Gasquet, D., Liégeois, J. P., Arai, S., Gahlan, H. A., Ahmed, H., Ishida, Y., Ikenne, M. (2017). The Ediacaran volcanic rocks and associated mafic dykes of the Ouarzazate Group (Anti-Atlas, Morocco): Clinopyroxene composition, whole-rock geochemistry and Sr-Nd isotopes constraints from the Ouzellarh-

Siroua salient (Tifnoute valley). Journal of African Earth Sciences. 127, 113-135. https://doi.org/10.1016/j.jafrearsci.2016.08.002.
12. Blein, O., Chevremont, P., Baudin, T., Hafid, A., Admou, H., Soulaimani, A., Ouanaimi, H, Bouabdelli, M., Gasquet, D., Padel, M. (2022). Contrasting Paleoproterozoic granitoids in the Kerdous, Tagragrad'Akka, Agadir-Melloul and Iguerda inliers (western Anti-Atlas, Morocco). Journal of African Earth Sciences. 189, 104500. https://doi.org/10.1016/j.jafrearsci.2022.104500.
13. Bouladon, J., Jouravsky, G., Morin, P. (1950). Etude préliminaire des pegmatites a muscovite et b´eryl du Sud de la Plaine de Tazenakht. Notes Mem. Serv. Geol. Maroc. 3 (n◦ 76), 207–235.
14. Bouougri, E. H., Lahna, A. A., Tassinari, C. C., Basei, M. A., Youbi, N., Admou, H., Saquaque, A., Boumehdi, M., A., Maacha, L. (2020). Time constraints on Early Tonian Rifting and Cryogenian Arc terrane-continent convergence along the northern margin of the West African craton: Insights from SHRIMP and LA-ICP-MS zircon geochronology in the Pan-African Anti-Atlas belt (Morocco). Gondwana Research. 85, 169-188. https://doi.org/10.1016/j.gr.2020.03.011.
15. Černý, P. (1991). Rare-element granitic pegmatites. Part I: Anatomy and internal evolution of pegmatite deposits. Geoscience Canada, 18(2), 49-67.
16. Černý, P., &Ercit, T. S. (1989). Mineralogy of niobium and tantalum: crystal chemical relationships, paragenetic aspects and their economic implications. In Lanthanides, Tantalum and Niobium: Mineralogy, Geochemistry, Characteristics of Primary Ore Deposits, Prospecting, Processing and Applications Proceedings of a workshop in Berlin, November 1986 (pp. 27-79). Springer Berlin Heidelberg.
17. Černý, P., Meintzer, R. E., Taylor, R. P., & Strong, D. F. (1988). Fertile granites in the Archean and Proterozoic fields of rare-element pegmatites: crustal environment, geochemistry and petrogenetic relationships. Recent Advances in the Geology of Granite-related Mineral Deposits. Canadian Institute of Mining and Metallurgy, Special Publication, 39, 170-206.
18. Cheilletz, A., Levresse, G., Gasquet, D., Azizi-Samir, M., Zyadi, R., Archibald, D. A., Farrar, E. (2002). The giant Imiter silver deposit: Neoproterozoic epithermal mineralization in the Anti-Atlas, Morocco. Mineralium Deposita. 37(8), 772-781. https://doi.org/10.1007/s00126-002-0317-0.
19. Chen, Y.W., Hu, R.Z., Bi, X.W., Luo, J.C. (2019). Genesis of the Guangshigou pegmatite type uranium deposit in the North Qinling Orogenic Belt, China. Ore Geol. Rev. 115, 103165.
20. Chèvremont, P., Blein, O., Razin, P., Baudin, T., Barbanson, L., Gasquet, D., Soulaimani, A., Admou, H., Youbi, N., Bouabdelli, M. (2013). Notice explicative carte géol. Maroc (1/50 000), feuille Bou Azer. Notes et Mémoires Serv. Géol. Maroc. 535bis.
21. Choubert, G. (1963). Histoire géologique du Précambrien de l'Anti-Atlas, tome 1, Notes et Mémoires du Service Géologique du Maroc. 162, 1– 352.
22. Clauer, N. (1974). Utilisation de la méthode rubidium-strontium pour la datation d'une schistosité de sédiments peu métamorphises : application au Précambrien II de la boutonnière de Bou Azzer-El Graara (Anti-Atlas, Maroc). Earth and Planetary Science Letters. 22(4), 404-412. https://doi.org/10.1016/0012-821X(74)90151-4.
23. Clauer, N. (1976). Géochimie isotopique du strontium des milieux sédimentaires. Application à la géochronologie de la couverture du craton ouest-africain. Sciences Géologiques Mémoires. 45, 256 p.
24. Cuney, M., Linnen, R.L. (2005). Granite-related rare-elementdeposits and experimentalconstraints on Ta-Nb-W-Sn-Zr-Hf mineralization. in Linnen R.L. and Samson I.M., eds., rare-element geochemistry and mineral deposits. Geological Association of Canada, GAC, Short Course, Canada. ⟨hal-00022536⟩.
25. Diallo, M., Bouabdellah, M., Levresse, G., Yans, J., Castorina, F., Klügel, A., ... &Maacha, L. (2021). Mineralogy, fluid inclusion, and Co-Sr isotope geochemistry to unravel the evolution of the magmatic-hydrothermal system at the Igoudrane Silver-Rich Deposit (Imiter District, Eastern Anti-Atlas, Morocco). Minerals, 11(9), 997.
26. Dill, H. G. (2015). Pegmatites and aplites: Their genetic and applied ore geology. Ore Geology Reviews, 69, 417-561.
27. El Bahat, A., Ikenne, M., Söderlund, U., Cousens, B., Youbi, N., Ernst, R., ... &Hafid, A. (2013). U–Pb baddeleyite ages and geochemistry of dolerite dykes in the Bas Drâa Inlier of the Anti-Atlas of Morocco: newly identified 1380 Ma event in the West African Craton. Lithos, 174, 85-98.
28. Ennih, N., Liégeois, J. P. (2001). The Moroccan Anti-Atlas: The West African craton passive margin with limited Pan-African activity. Implications for the northern limit of the craton. Precambrian Research. 112(3-4), 289-302. https://doi.org/10.1016/S0301-9268(01)00195-4.
29. Ennih, N., Liégeois, J. P. (2008). The boundaries of the West African craton, with special reference to the basement of the Moroccan metacratonic Anti-Atlas belt. Geological Society, London, Special Publications. 297(1), 1-17. https://doi.org/10.1144/SP297.1.

30. Errami, E., Bonin, B., Laduron, D., Lasri, L. (2009). Petrology and geodynamic significance of the post-collisional Pan-African magmatism in the Eastern Saghro area (Anti-Atlas, Morocco). Journal of African Earth Sciences. 55(1-2), 105-124. https://doi.org/10.1016/j.jafrearsci.2009.02.006.
31. Essarraj, S., Boiron, M. C., Cathelineau, M., Tarantola, A., Leisen, M., Boulvais, P., &Maacha, L. (2016). Basinal brines at the origin of the Imiter Ag-Hg deposit (Anti-Atlas, Morocco): Evidence from LA-ICP-MS data on fluid inclusions, halogen signatures, and stable isotopes (H, C, O). Economic Geology, 111(7), 1753-1781.
32. Fekkak, A., Pouclet, A., Badra, L. (2002). The pre-Pan-African rifting of Saghro (Anti-Atlas, Morocco): example of the middle Neoproterozoic basin of Boumalne. Bulletin de la Société géologique de France. 173(1), 25-35.
33. Fekkak, A., Pouclet, A., Ouguir, H., Ouazzani, H., Badra, L., Gasquet, D. (2001). Géochimie et signification géotectonique des volcanites du Cryogénien inférieur du Saghro (Anti-Atlas oriental, Maroc) /Geochemistry and geotectonicsignificance of EarlyCryogenianvolcanics of Saghro (Eastern Anti-Atlas, Morocco). Geodinamica Acta. 14(6), 373-385. https://doi.org/10.1080/09853111.2001.10510730.
34. Franz, G., &Liebscher, A. (2004). Physical and chemical properties of the epidote minerals–an introduction–. Reviews in mineralogy and geochemistry, 56(1), 1-81.
35. Gasquet, D., Chèvremont, P., Baudin, T., Chalot-Prat, F., Guerrot, C., Cocherie, A., Roger, J., Hassenforder, B., Cheilletz, A. (2004). Polycyclic magmatism in the Tagragrad'Akka and Kerdous–Tafeltast inliers (Western Anti-Atlas, Morocco). Journal of African Earth Sciences. 39(3-5), 267-275. https://doi.org/10.1016/j.jafrearsci.2004.07.062.
36. Gasquet, D., Ennih, N., Liégeois, J.P., Soulaimani, A., Michard, A. (2008). The Pan-African Belt. In: Michard, et al. (Ed.), Continental evolution: The Geology of Morocco.: Lecture Notes in Earth Sciences, 116. Springer Verlag, Berlin, pp. 33–64.
37. Gasquet, D., Levresse, G., Cheilletz, A., Azizi-Samir, M. R., Mouttaqi, A. (2005). Contribution to a geodynamic reconstruction of the Anti-Atlas (Morocco) during Pan-African times with the emphasis on inversion tectonics and metallogenic activity at the Precambrian–Cambrian transition. Precambrian Research. 140(3-4), 157-182. https://doi.org/10.1016/j.precamres.2005.06.009.
38. Guilbert, J.M., and Park, C.F., Jr. (1986). The geology of oredeposits: New York, W.H. Freeman, 985 p.
39. Guillou, J. J., Monthel, J., Samama, J. C., Tijani, A. (1988). Morphologie et chronologie relative des associations minérales du gisement mercuro-argentifère d'Imiter (Anti-Atlas-Maroc). Notes et mémoires du Service géologique. 334, 215-228.
40. Hassenforder, B. (1987). La tectonique panafricaine et varisque de l'Anti-Atlas dans le massif du Kerdous (Maroc) (Doctoral dissertation, Strasbourg 1).
41. Hefferan, K., Samson, S., Hietpas, J., Admou, H., Inglis, J., Saquaque, A., Heywood, N. (2012). A ~604 Ma depositional age for the Tiddiline conglomerate, BouAzzer inlier, Morocco based on U-Pb dating of detrital zircon. Geol. Soc. Am. Abstr. Prog., 44, 285.
42. Hefferan, K., Soulaimani, A., Samson, S. D., Admou, H., Inglis, J., Saquaque, A., Chaib, L., Heywood, N., (2014). A reconsideration of Pan African orogenic cycle in the Anti-Atlas Mountains, Morocco. Journal of African Earth Sciences. 98, 34-46. https://doi.org/10.1016/j.jafrearsci.2014.03.007.
43. Hindermeyer, J. (1953). Découverte d'un affleurement de PI probable entre Ouarzazate et Skoura (Anti-Atlas marocain). Compte rendu sommaire des séances de la Société géologique de France. 3, 34-35.
44. Ikenne, M., Bekker, A., Ernst, R.E., Youbi, N., Ait Lahna, A., Soderlund, U., Tassinari, C.C. G., Ousbih, M., Boumehdi, M.A., Bensalah, M.K. (2021a). Discussion on "From Pan-African transpression to Cadomiantranstension at the West African margin : new U-Pb zircon ages from the Eastern Saghro Inlier (Anti-Atlas, Morocco)" by Errami et al. 2020 (Geol. Soc. London Spec. Publ 503, 209-233). J. Geol. Soc. 178.
45. Ikenne, M., Ennaciri, A., Ouguir, H., Cousens, B., Ziyadi, R., Mouhagir, M., El-Gaouzi, A. (2007). Geochemical signature and geodynamic significance of an Ag-Hg mineralized dyke swarm in the neoproterozoic inlier of imiter-Anti-Atlas (Morocco). Ofioliti. 32(2), 109-118. https://doi.org/10.4454/ofioliti.v32i2.351.
46. Ikenne, M., Mortaji, A., Gasquet, D., Stussi, J. M. 1(997). Les filons basiques des boutonnières du Bas Drâa et de la Tagragra d'Akka : témoins des distensions néoprotérozoïques de l'Anti-Atlas occidental (Maroc). Journal of African Earth Sciences. 25(2), 209-223.
47. Ikenne, M., Söderlund, U., Ernst, R. E., Pin, C., Youbi, N., Hafid, A. (2017). A c. 1710 Ma mafic sill emplaced into a quartzite and calcareous series from Ighrem, Anti-Atlas–Morocco: evidence that the Taghdout passive margin sedimentary group is nearly 1 Ga older than previously thought. Journal of African Earth Sciences. 127, 62-76. https://doi.org/10.1016/j.jafrearsci.2016.08.020.

48. Ikenne, M., Souhassou, M., Saintilan, N. J., Karfal, A., Hassani, A. E., Moundi, Y., Ousbih, M., Ezzghoudi, M., Zouhir, M., Maacha, L. (2021b). Cobalt–nickel–copper arsenide, sulfarsenide and sulfide mineralization in the BouAzzer window, Anti-Atlas, Morocco: one century of multi-disciplinary and geological investigations, mineral exploration and mining. Geological Society, London, Special Publications. 502(1), 45-66. https://doi.org/10.1144/SP502-2019-132.
49. Inglis, J. D., D'Lemos, R. S., Samson, S. D., Admou, H. (2005). Geochronological constraints on Late Precambrian intrusion, metamorphism, and tectonism in the Anti-Atlas Mountains. The Journal of geology. 113(4), 439-450. https://doi.org/10.1086/430242.
50. Inglis, J.D., Hefferan, K., Samson, S.D., Admou, H., Saquaque, A., 2017. Determining ageof Pan African metamorphism using Sm-Nd garnet-whole rock geochronology andphase equilibria modeling in the Tasriwine ophiolite, Sirwa, Anti-Atlas Morocco. J.Afr. Earth Sc. 127, 88–98.
51. Iwasaki, A., Fujisada, H., & Torii, M. (2001). ASTER initial image evaluation. In Sensors, Systems, and Next-Generation Satellites IV (Vol. 4169, pp. 56-66). SPIE.
52. Jahns, R. H., & Burnham, C. W. (1969). Experimental studies of pegmatite genesis; l, A model for the derivation and crystallization of granitic pegmatites. Economic Geology, 64(8), 843-864.
53. Kratt, C., Calvin, W. M., &Coolbaugh, M. F. (2010). Mineral mapping in the Pyramid Lake basin: Hydrothermal alteration, chemical precipitates and geothermal energy potential. Remote Sensing of Environment, 114(10), 2297-2304.
54. Kwak, T. A. P., & Abeysinghe, P. B. (1987). Rare earth and uranium minerals present as daughter crystals in fluid inclusions, Mary Kathleen U-REE skarn, Queensland, Australia. Mineralogical Magazine, 51(363), 665-670.
55. Leblanc, L. J., Morlok, E. K., &Pierskalla, W. P. (1975). An efficient approach to solving the road network equilibrium traffic assignment problem. Transportation research, 9(5), 309-318.
56. Leistel, J. M., Qadrouci, A. (1991). Le gisement argentifère d'Imiter (Protérozoïque supérieur de l'Anti-Atlas, Maroc). Contrôles des minéralisations, hypothèse génétique et perspectives pour l'exploration. Chronique de la recherche minière. (502), 5-22.
57. Levresse, G., Cheilletz, A., Gasquet, D., Reisberg, L., Deloule, E., Marty, B., Kyser, K. (2004). Osmium, sulphur, and helium isotopic results from the giant Neoproterozoic epithermal Imitersilver deposit, Morocco: evidence for a mantle source. Chemical geology. 207(1-2), 59-79. https://doi.org/10.1016/j.chemgeo.2004.02.004.
58. Liégeois, J. P., Fekkak, A., Bruguier, O., Errami, E., Ennih, N. (2006). The Lower Ediacaran (630–610 Ma) Saghro group: an orogenic transgressive basin development during the early metacratonic evolution of the Anti-Atlas (Morocco). In: IGCP485 4th meeting, Algiers, p. 57.
59. Linnen, R.L., van Lichtervelde, M., Černý, P. (2012). Granitic pegmatites as sources of strategic metals. Elements 8, 275–280.
60. Liu, Y., Gao, J. F., Qi, L., & Min, K. (2023). Textural and compositional variation of mica from the Dexing porphyry Cu deposit: constraints on the behavior of halogens in porphyry systems. Acta Geochimica, 42(2), 221-240.
61. London, D. (2016b). Rare-element Granitic Pegmatites. In: Verplanck, P.L., Hitzman, M.W. (Eds.), Rare Earth and Critical Elements in Major Deposit Types, Reviews in Economic Geology. Society of Economic Geologists, Inc, Littleton, CO, 18, pp. 165–193.
62. Lowell, J.D, Guilbert, J.M. (1970). Lateral and vertical alterationmineralization zoning in porphyry ore deposits: Econ. Geol. Bull. Soc. Econ. Geol., 65(4): 373-408.
63. Mariano A. N. (1989). Economic geology of rare earth elements. In Geochemistry and Mineralogy of Rare Earth Elements, pp. 309-337. Rev. Mineral. 21. Mineral Soc. Am.
64. Massironi, M., Bertoldi, L., Calafa, P., Visonà, D., Bistacchi, A., Giardino, C., Schiavo, A. (2008). Interpretation and processing of ASTER data for geological mapping and granitoids detection in the Saghro massif (Eastern Anti-Atlas, Morocco) Interpretation of ASTER data for geological mapping and granitoids detection. Geosphere. 4(4), 736-759. https://doi.org/10.1130/GES00161.1.
65. Massironi, M., Moratti, G., Algouti, A. H., Benvenuti, M., Dal Piaz, G. V., Eddebbi, A., Boukhari, A., Laftouhi, N. E., Ouanaimi, H., Schiavo, A., Taj Eddine, K., Visonà, D. (2007). Carte géologique du Maroc au 1/50 000, feuille Boumalne. Notes et Mémoires du Service Géologique du Maroc. 521 bis.
66. Mazdab, F. K., Wooden, J. L., & Barth, A. P. (2007). Trace element variability in titanite from diverse geologic environments. In Geological Society of America, Abstracts with Programs, Vol. 39, p. 406.
67. Morin, P. (1952). Mica et beryl. Chap. XVII. In : Geologie des gites mineraux marocains. Notes et Mem. Serv, vol. 87. Geol. Maroc, pp. 337–346

68. Morsli, Y., Zerhouni, Y., Maimouni, S., Alikouss, S., Kadir, H., &Baroudi, Z. (2021). Pegmatite mapping using spectroradiometry and ASTER data (Zenaga, Central Anti-Atlas, Morocco). Journal of African Earth Sciences, 177, 104153.
69. Morsli, Y., Zerhouni, Y., Wafik, A., Elouazzani, A., Alikouss, S., Saidi, A., & Baroudi, Z. (2022). Eburneen pegmatites of the Zenaga inlier (Anti-Atlas, Morocco): Petrography, geochemistry, and classification. Journal of African Earth Sciences, 186, 104438.
70. Mortaji, A., Ikenne, M., Gasquet, D., Barbey, P., &Stussi, J. M. (2000). Palaeoproterozoic granitoids from the Bas Draa and Tagragrad'Akka Inliers (western Anti-Atlas, Morocco): part of the jigsaw puzzle concerning the West African Craton. J Afr Earth Sci, 31, 523-538.
71. Morteani, G., &Gaupp, R. (1989). Geochemical evaluation of the tantalum potential of pegmatites. In Lanthanides, Tantalum and Niobium: Mineralogy, Geochemistry, Characteristics of Primary Ore Deposits, Prospecting, Processing and Applications Proceedings of a workshop in Berlin, November 1986 (pp. 303-310). Springer Berlin Heidelberg.
72. Ninomiya, Y. (2016). Lithologic mapping with multispectral ASTER TIR and SWIR data. Proc. SPIE 5234. https://doi.org/10.1117/12.511902.
73. Oliver, N. H. S., Pearson, P. J., Holcombe, R. J., & Ord, A. (1999). Mary Kathleen metamorphic-hydrothermal uranium—rare-earth element deposit: Ore genesis and numerical model of coupled deformation and fluid flow. Australian Journal of Earth Sciences, 46(3), 467-484.
74. Ouguir, H. (1997). Contexte géologique du gisement argentifère d'Imiter (Anti-Atlas oriental, Maroc). Contrôle volcanique et structural de la mise en place des concentrations métalliques à Ag-Hg. Unpublished Thesis. University of Meknes, 215 p.
75. Ouguir, H., Macaudière, J., Dagallier, G. (1996). Le Protérozoïque supérieur d'Imiter, Saghro oriental, Maroc : un contexte géodynamique d'arrière-arc. Journal of African Earth Sciences. 22(2), 173-189. https://doi.org/10.1016/0899-5362(96)00002-4.
76. Ouguir, H., Macaudiere, J., Dagallier, G., Qadrouci, A., Leistel, J. M. (1994). Cadre structural du gite Ag-Hg d'Imiter (Anti Atlas, Maroc) ; implication metallogenique. Bulletin de la Société géologique de France. 165(3), 233-248.
77. Palinkaš, S. S., Wegner, R., Čobić, A., Palinkaš, L. A., Barreto, S. D. B., Váczi, T., &Bermanec, V. (2014). The role of magmatic and hydrothermal processes in the evolution of Be-bearing pegmatites: Evidence from beryl and its breakdown products. American Mineralogist, 99(2-3), 424-432.
78. Pan, Y., Fleet, M. E., &MacRae, N. D. (1993a). Late alteration in titanite ($CaTiSiO_5$): redistribution and remobilization of rare earth elements and implications for U/Pb and Th/Pb geochronology and nuclear waste disposal. Geochimica et Cosmochimica Acta, 57(2), 355-367.
79. Pan, Y., Fleet, M. E., & Macrae, N. D. (1993b). Oriented monazite inclusions in apatite porphyroblasts from the Hemlo gold deposit, Ontario, Canada. Mineralogical Magazine, 57(389), 697-707.
80. Permingeat, F. (1955). Surlesniobo-tantalates de l'Anti-Atlas, Maroc : tapiolite et columbite. Bull. Soc. Fr. Mineral. Cristallogr. 78, 123–156.
81. Pour, B.A., Hashim, M., Pournamdari, M. (2015). Chromitite prospecting using Landsat TM and ASTER remote sensing data. In: Isprs Annals of the Photogrammetry, Remote Sensing and Spatial Information Sciences, Volume Ii-2/W2, 2015 Joint International Geoinformation Conference 2015, 28–30 October 2015. Kuala Lumpur, Malaysia.
82. Rajendran, S., Nasir, S., Kusky, T.M., Ghulam, A., Gabr, S., El Gali, M. (2013). Detection of hydrothermal mineralized zones associated with listwaenites rocks in the Central Oman using ASTER data. Ore Geol. Rev. 53, 470–488.
83. Ranjbar, H., Masoumi, F., & Carranza, E. J. M. (2011). Evaluation of geophysics and spaceborne multispectral data for alteration mapping in the Sar Cheshmeh mining area, Iran. International Journal of Remote Sensing, 32(12), 3309-3327.
84. Rowan, L. C., & Mars, J. C. (2003). Lithologic mapping in the Mountain Pass, California area using advanced spaceborne thermal emission and reflection radiometer (ASTER) data. Remote sensing of Environment, 84(3), 350-366.
85. Sadeghi, M., Jones, S. B., & Philpot, W. D. (2015). A linear physically-based model for remote sensing of soil moisture using short wave infrared bands. Remote Sensing of Environment, 164, 66-76.
86. Samson, S. D., Inglis, J. D., D'lemos, R. S., Admou, H., Blichert-Toft, J., Hefferan, K. (2004). Geochronological, geochemical, and Nd–Hf isotopic constraints on the origin of Neoproterozoic plagiogranites in the Tasriwine ophiolite, Anti-Atlas orogen, Morocco. Precambrian Research. 135 (1-2), 133-147. https://doi.org/10.1016/j.precamres.2004.08.003.

87. Saquaque, A., Admou, H., Karson, J., Hefferan, K., Reuber, I. (1989). Precambrian accretionary tectonics in the BouAzzer-El Graara region, Anti-Atlas, Morocco. Geology. 17(12), 1107-1110. https://doi.org/10.1130/0091-7613(1989)017<1107:PATITB>2.3.CO;2.
88. Shabou, M., Mougenot, B., Lili Chabaane, Z., Walter, C., Boulet, G., Ben Aissa, N., &Zribi, M. (2015). Soil clay content mapping using a time series of Landsat TM data in semi-arid lands. Remote sensing, 7(5), 6059-6078.
89. Simmons, W.B., Webber, K.L., Falster, A.U., Nizamoff, J.W. (2003). Pegmatology —Pegmatite Mineralogy, Petrology and Petrogenesis. Rubellite Press, New Orleans, LA
90. Soe, M., Kyaw, T. A., & Takashima, I. (2005). Application of remote sensing techniques on iron oxide detection from ASTER and Landsat images of Tanintharyi coastal area, Myanmar.
91. Testa, F. J., Villanueva, C., Cooke, D. R., & Zhang, L. (2018). Lithological and hydrothermal alteration mapping of epithermal, porphyry and tourmaline breccia districts in the Argentine Andes using ASTER imagery. Remote Sensing, 10(2), 203.
92. Thomas, R. J., Chevallier, L. P., Gresse, P. G., Harmer, R. E., Eglington, B. M., Armstrong, R. A., De Beer, H., Martini, J. E. J., De Kock, G. S., Macey, P. H., Ingram, B. A. (2002). Precambrian evolution of the Sirwa window, Anti-Atlas orogen, Morocco. Precambrian Research. 118(1-2), 1-57. https://doi.org/10.1016/S0301-9268(02)00075-X.
93. Thomas, R. J., Fekkak, A., Ennih, N., Errami, E., Loughlin, S. C., Gresse, P. G., Chevallier, L. P., Liégeois, J. P. (2004). A new lithostratigraphic framework for the Anti-Atlas Orogen, Morocco. Journal of African Earth Sciences. 39(3-5), 217-226. https://doi.org/10.1016/j.jafrearsci.2004.07.046.
94. Toummite, A., Liégeois, J. P., Gasquet, D., Bruguier, O., Beraaouz, E. H., Ikenne, M. (2013). Field, geochemistry and Sr-Nd isotopes of the Pan-African granitoids from the Tifnoute Valley (Sirwa, Anti-Atlas, Morocco): a post-collisional event in a metacratonic setting. Mineralogy and Petrology. 107(5), 739-763. https://doi.org/10.1007/s00710-012-0245-3.
95. Triantafyllou, A., Berger, J., Baele, J. M., Mattielli, N., Ducea, M. N., Sterckx, S., Samson, S., Hodel, F., Ennih, N. (2020). Episodic magmatism during the growth of a Neoproterozoic oceanic arc (Anti-Atlas, Morocco). Precambrian Research. 339, 105610. https://doi.org/10.1016/j.precamres.2020.105610.
96. Wang, S., & Williams, P. J. (2001). Geochemistry and origin of Proterozoic skarns at the Mount Elliott Cu–Au (–Co–Ni) deposit, Cloncurry district, NW Queensland, Australia. Mineralium Deposita, 36, 109-124.
97. Wise, M. A. (2019). The petrologic significance of epidote in granitic pegmatites. The Canadian Mineralogist, 57(5), 817-819.
98. Zamyad, M., Afzal, P., Pourkermani, M., Nouri, R., & Jafari, M. R. (2019). Determination of hydrothermal alteration zones using remote sensing methods in Tirka Area, Toroud, NE Iran. Journal of the Indian Society of Remote Sensing, 47, 1817-1830.
99. Zoheir, B., &Emam, A. (2014). Field and ASTER imagery data for the setting of gold mineralization in Western Allaqi–Heiani belt, Egypt: A case study from the Haimur deposit. Journal of African Earth Sciences, 99, 150-164.